



PERGAMON

Vision Research 42 (2002) 2419–2430

---



---

**Vision  
Research**


---



---

www.elsevier.com/locate/visres

# Speed of response initiation in a time-to-contact discrimination task reflects the use of $\eta$

Joan López-Moliner<sup>a,\*</sup>, Claude Bonnet<sup>b</sup>

<sup>a</sup> *Departament de Psicologia Bàsica, Evolutiva i Educació, Facultat de Psicologia, Universitat Autònoma de Barcelona, 08193 Cerdanyola, Barcelona, Catalonia, Spain*

<sup>b</sup> *Laboratoire des Systèmes Biomécaniques et Cognitifs, Université Louis Pasteur, IMFS UMR 7507 du CNRS, Strasbourg, France*

Received 8 November 2001; received in revised form 15 May 2002

---

## Abstract

Avoiding collisions and making interceptions seem to require an organism to estimate the time that will elapse before an object will arrive to the point of observation (time-to-contact). The most outstanding account for precise timing has been the tau hypothesis. However, recent studies demonstrate that tau is not the only source of information in judging time-to-contact. By measuring reaction time in a time-to-contact discrimination task, we show that the  $\eta$  function, which is a specific combination of optical size and rate of expansion, explains both accuracy and the observed RT pattern. The results conform to the hypothesis that the observers initiate the response when  $\eta$  reaches a response threshold value.

© 2002 Elsevier Science Ltd. All rights reserved.

*Keywords:* Motion in depth; Time-to-contact; Optical variables; Response threshold

---

## 1. Introduction

Avoiding undesirable collisions or making interceptions are very relevant visually guided actions. They seem to require an organism to estimate the time that will elapse before an object will arrive to the point of observation (time-to-contact). However, which sources of information are involved in time-to-contact (TC) estimation is still an open question. The most outstanding account for the timing of interceptive actions has been based on the tau ( $\tau$ ) parameter, which was framed within Gibson's ecological approach to perception.  $\tau$  can specify an object's TC and its appeal has been motivated by its simple computation: the ratio of object's image size to its rate of expansion. Psychophysical support for  $\tau$  has convincingly been reported in carefully controlled experiments (e.g. Regan & Hamstra, 1993; Regan & Vincent, 1995), when no other visual cues were available. However, other non-psychophysically oriented studies with, in general, untrained subjects have shown that other information is used instead of, or in addition to,  $\tau$  (e.g. DeLucia, 1991; DeLucia, 1999; Kerzel,

Hecht, & Kim, 1999; Smeets, Brenner, Trébuchet, & Mestre, 1996; Wann, 1996).

Recently, Sun and Frost (1998) have depicted a more complex mosaic of different mechanisms for TC computation implemented in natural visual systems that could account for an optimal timing of action. They have identified four kinds of optical computation based on the temporal response patterns of looming sensitive neurons in the nucleus rotundus of pigeons. Some computations would simply track the temporal pattern of the two optical variables: optical size ( $\theta$ ) and its rate of change, that is the rate of expansion ( $\dot{\theta}$ ), see Fig. 1A. Both  $\theta$  and  $\dot{\theta}$  increase hyperbolically with time. These two optical variables can be combined in different ways to give place to higher order computations. One example is  $\tau$  or its inverse,  $\tau^{-1}$ , which are plotted in Fig. 1B. While  $\tau^{-1}$  increases hyperbolically,  $\tau$  decreases linearly with time. The response pattern of neurons sensitive to  $\tau$  (or  $\tau^{-1}$ ) is not affected by changes in physical size and approaching velocity. Yet another computation resulting from combining  $\theta$  and  $\dot{\theta}$  is shown in Fig. 1B. This function, called eta ( $\eta$ ), was proposed by Hatsopoulos, Gabbiani, and Laurent (1995) to model locusts' looming-detector responses and can be described as a function of time as follows:

\* Corresponding author.

E-mail address: [joan.lopez.moliner@uab.es](mailto:joan.lopez.moliner@uab.es) (J. López-Moliner).

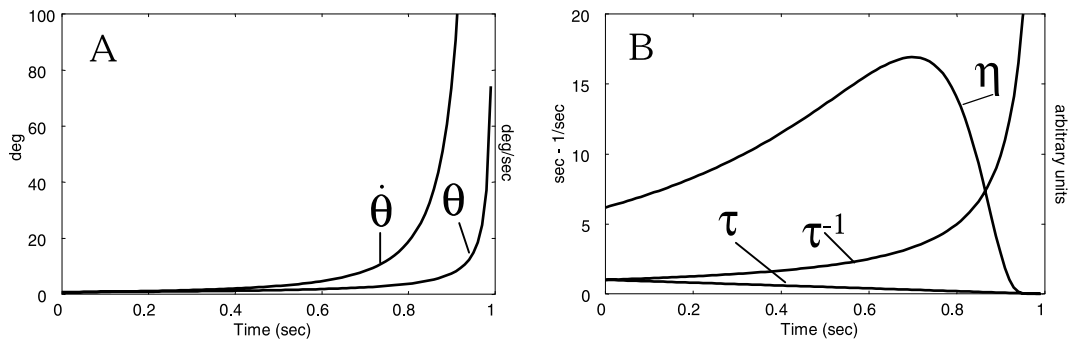


Fig. 1. (A) Optical size ( $\theta$ ) and its first time derivative, the angular rate of expansion ( $\dot{\theta}$ ) as a function of time. (B)  $\tau$ ,  $\tau^{-1}$  and  $\eta$  plotted as a function of time. In (A) and (B) 0 on the abscissa corresponds to the initial time  $t = 0$  and 1 to contact time  $TC = 1$  s.

$$\eta_t = C \times \dot{\theta}_t \times e^{-\alpha\theta_t} \quad (1)$$

where  $C$  is a constant that modulates the overall magnitude of the neuron's response and  $\alpha$  is a parameter that prevents the neuron from being saturated close to the collision due to a very large excitatory response.  $\eta$  has an ascending phase which slope is inversely proportional to object's optical size. As can be noted,  $\eta$  function has a peak before the collision occurs. Larger objects reach this peak earlier than smaller approaching objects moving at the same speed.

In a recent study, Smith, Flach, Dittman, and Starnard (2001) have shown how a linear combination of  $\theta$  and  $\dot{\theta}$  can satisfactorily model the pattern of results in a timing task.  $\theta$  and  $\dot{\theta}$  would be flexibly combined in order to meet task requirements. In sum, it seems that the visual system can be tuned to optical size ( $\theta$ ), to rate of expansion ( $\dot{\theta}$ ), to  $\tau$  or  $\tau^{-1}$  or to some other combination of the two optical variables  $\theta$  and  $\dot{\theta}$ .  $\eta$  and a weighted sum of  $\theta$  and  $\dot{\theta}$  would be examples of the latter case. Each one of these computations provides different information about an object's approaching course and an organism possibly responds on the basis of these different functions (Laurent & Gabbiani, 1998). As long as a looming pattern could imply an impending collision, it may be useful that a signal that carries TC information gets larger as collision approaches (Koenderink, 1985). This is not the case of  $\tau$ . Moreover, it is not clear how the nervous system could represent TC in units of time (Tresilian, 1999). Therefore,  $\tau$  does not seem, a priori, the best candidate for response initiation. This paper aims at addressing which information is (or are) used by the visual system to initiate a motor response.

In spite of the different models of TC measurement that have been put forward (see Tresilian, 1999, for a recent revision), most of the studies have focused on the distribution of type of response across a given dimension (e.g. time, angular velocity) in order to see whether its shape reflects the use of a certain function, often  $\tau$ . Thus, possible meaningful relations between variables such as those described above and the speed of response

initiation have been missed. Few empirical data on which optical variables lead to response initiation is available. Rushton and Wann (1999) found that the response was initiated by the optical cue that signals the earliest arrival time, but systematic studies on which sensory information, if any, modulates the speed of response initiation have not been reported so far.

Precise reaction time (RT) measurements within the bounds of a psychophysical method would allow one to relate the speed of processing to the intensity values of optical variables (or combination of them). Most RT models assume an accumulation process of sensory information in time. When stimulus intensity increases, the rate of accumulation increases stochastically until a response threshold level is reached (e.g. Bonnet & Dresch, 2001; Link, 1992). The neuron's firing rate biologically supports this mechanism. Hanes and Schall (1996) found that the distribution of RT could be accounted for by the stochastic variability in the growing rate of neural activity towards the threshold, confirming this type of link between neuron's activity and motor behavior. Looking at the psychophysical side, it has been shown that both simple RT and choice RT decrease as a power function of stimulus intensity (Pins & Bonnet, 1996). This function is called Piéron function. However, due to the duration and variability of observed RTs, decision processes should intervene somewhat, adding an extra time to the sensorial and motor delays. Pins and Bonnet (2000) showed that uncertainty lengthens RT faster in the threshold region than in suprathreshold ranges. Thus, by using suprathreshold ranges, variations of the mean RT should be accounted for by variations in stimulus intensity, assuming the subject's response criterion remains constant. Trained subjects can be used to minimize response factors.

In order to determine which optical variable, or combination of them, is responsible for the speed of processing in a TC discrimination task we can fit different theoretical RT functions to the observed RT data. The ratio of the object's physical size ( $S$ ) to its physical approaching velocity ( $v$ ) is very useful for this purpose.

Distinct RT functions can be mathematically derived as a function of the ratio of size to velocity ( $S/v$ ) (Sun & Frost, 1998). The form of the RT function with the best fit to the observed RT distribution would allow one to elucidate which optical variable (or combination of them) triggers the response. For example, if the response is triggered when  $\tau$  (or  $\tau^{-1}$ ) reaches a response threshold then we expect the RT data points to lie along a flat curve. Note that  $\tau$  (or its inverse) is invariant over changes in size ( $S$ ) and velocity ( $v$ ). In contrast, if  $\theta$  is the variable that modulates subject's response, then the RT data points will not significantly deviate from a function that declines linearly with  $S/v$ . Predictions can also be made for  $\dot{\theta}$ , for a weighted sum of  $\theta$  and  $\dot{\theta}$  and for  $\eta$ .

## 2. Experiment 1: determining the threshold region in TC discrimination

This experiment consisted in a relative TC discrimination task and was performed by all observers before carrying out the RT experiment. Experiment 1 aimed at (1) obtaining the discrimination thresholds for relative TC between two objects for each of the subjects, in order to use appropriate suprathreshold values in Experiment 2, (2) determining the optical variables that the observers used to base their responses. Specifically, this experiment aimed at ensuring that the observers were not prone to bias by using differences in rate of expansion or size change instead of differences in arrival time.

### 2.1. Subjects

Two trained subjects, JM (author) and ET, and one less trained subject (EN) took part in the experiment. JM had normal vision, ET and EN had corrected-to-normal vision.

### 2.2. Apparatus and stimuli

The stimuli were generated by a PC (Pentium-II 400 MHz) and were displayed on a high-resolution monitor ( $1280 \times 1024$  pixels) at a frame rate of 85 Hz in synchrony with the monitor refresh rate. The screen (EIZO FlexScan F77 21-in.) was viewed monocularly from 60 cm and the unused eye was patched. At that distance the display subtended  $36.92 \times 27.69$  deg. The luminance of the stimuli (solid sharp-edged squares) was  $40 \text{ cd m}^{-2}$  and they were superimposed on a black background ( $0.3 \text{ cd m}^{-2}$ ). The square's angular subtense was varied through time according to the following expression (see Regan & Hamstra, 1993, for a complete derivation):

$$\tan \theta_t = \frac{\tan \theta_0}{1 - t/T_0} \quad (2)$$

where  $\theta_0$  is the starting size and  $T_0$  the designated time-to-contact.

### 2.3. Procedure

A temporal two-alternative forced-choice (2AFC) paradigm was used in conjunction with the weighted up-down method proposed by Kaernbach (1991). On each trial two solid squares were presented sequentially separated by an interval of 400 ms. The first square (standard square) had the standard time-to-contact (1.0 s) and the time-to-contact of the second square (comparison square) was varied across trials on the basis of the staircase procedure. The presentation time of the two expanding squares was varied independently to remove size increment ( $\Delta\theta$ ) as a reliable cue. The presentation time was set randomly in the range 440–660 ms on a trial-to-trial basis.

The subjects had to signal, by pressing one of two buttons, if the second square would arrive sooner than or later than the first square to the point of observation. As stated by Gray and Regan (1998), several staircases have to be interleaved in order to prevent the subjects from anticipating variations in time-to-contact and to determine on which optical variables the subjects based their responses. In a given run we interleaved four initial rates of expansion (0.577, 0.658, 0.855 and 0.975 deg/s) for the comparison square and two different starting values of time-to-contact for the comparison square, one for which the subject had to press the “sooner than” button and other for the “later than” button. Each observer carried out four runs. The standard square had an initial rate of expansion of 0.75 deg/s. The two initial values of time-to-contact for the comparison square were  $\pm 15\%$  of the standard TC (1 s) and the step size was set to 0.01 s. The combination of these values resulted in eight independent staircases. The four “sooner than” staircases and the four “later than” staircases converged on 75% and 25% “sooner than” responses respectively. A run was ended after 10 reversals (change from “sooner” to “later” or vice versa) in each of the eight staircases. The mean of the last eight reversals was taken as the convergence point. The differential threshold (DT) was defined as the half difference between the 0.75% and 0.25% estimates and the relative differential threshold was the ratio of DT to the mean of the 0.25 and 0.75 levels.

### 2.4. Results

Fig. 2 shows the relative differential threshold (Weber fraction) in discriminating time-to-contact versus the initial rate of expansion. Data points for the three observers are plotted separately. Data shows that the initial rate of expansion had no effect on estimates. Had the observers' responses been affected by the rate of

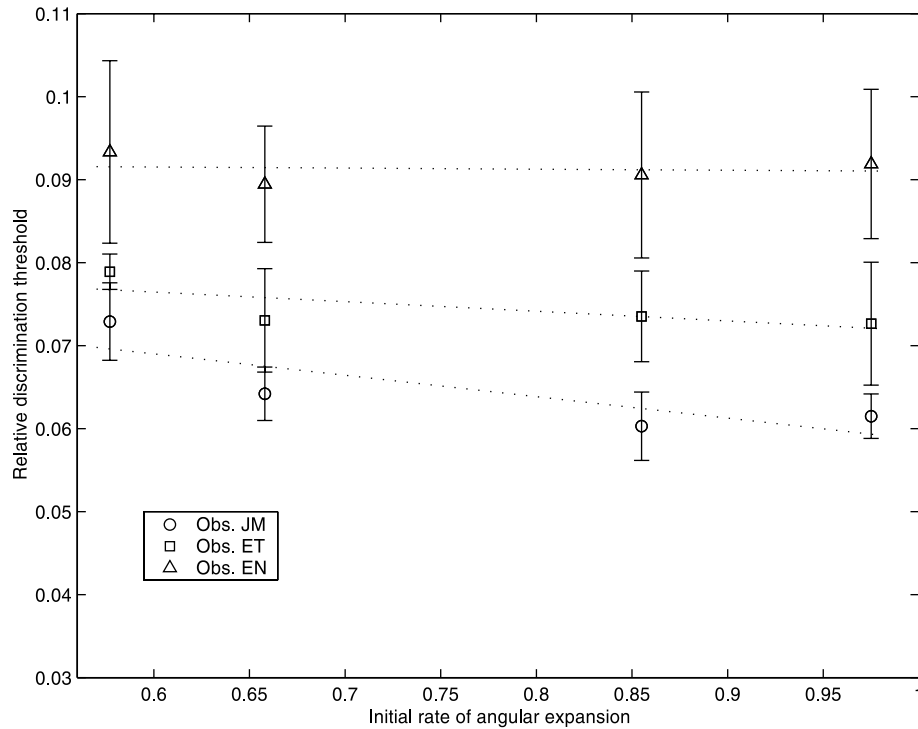


Fig. 2. Relative differential thresholds (Weber fractions) were plotted versus initial rate of angular expansion of the comparison object. 0.75 on the abscissa corresponds to the initial rate of expansion of the standard object. Bars show  $\pm 1$  SE.

expansion the estimates for different initial rates of expansion would have been significantly different. We fitted a linear function to the data points for each observer separately and the coefficients were not significantly different from zero (Observer JM:  $t = -2.061$ ,  $p = 0.174$ ; Observer ET:  $t = -1.4571$ ,  $p = 0.2825$ ; Observer EN:  $t = -0.199$ ,  $p = 0.861$ ). The intercept was very similar for the two trained subjects, 0.0845 and 0.0834 for JM and ET respectively, while for EN was 0.0923.

The just-noticeable difference in TC ranges from 6.0% to 10% and it is in accordance with previous results (e.g. Gray & Regan, 1998; Regan & Hamstra, 1993). Consequently, in the second experiment, the smallest difference in TC between the standard stimulus and the comparison stimulus will be above 10% for all the observers.

### 3. Experiment 2

As stated in Section 1, the goal of this experiment is to elucidate which optical variable (or combination of them) is responsible for the response initiation. When discriminating TC between two stimuli, they generate a sequence of signals, optical information, which vary continuously. The response can be given at any moment during the path of the second stimulus. According to

Link's model (Link, 1992), the response should be initiated at the moment when the difference in the relevant signal reaches a response threshold. In order to generate a form of internalized reference time to which compare the stimuli, we relied on a modification of the procedure employed by Regan and Hamstra (1993). Observers had to indicate if a second target would arrive at the observation point earlier or later than a previous object with a standard arrival time. Todd (1981) reported a study on TC discrimination with two simultaneously presented approaching objects. However, we decided to use a discrimination task with suprathreshold stimuli presented successively instead of two simultaneous objects. The reason for this is threefold. First, selective attention has proved to be necessary in order to estimate TC properly (Gray, 2000). Had we used two simultaneous objects an additional source of RT variability would have been necessary to account for attentional shifts, thereby rendering difficult posterior parameter interpretation. Second, although it seems possible that relative judgment tasks minimize the influence of cognitive factors (Tresilian, 1995), DeLucia (1991) showed a response bias towards the object with a larger image in a study with two simultaneous objects. Finally, the procedure introduced by Regan and Hamstra has proven to be adequate to dissociate several sources of information (e.g. rate of expansion, size increment) which could confound discrimination measurements.

### 3.1. Subjects

The same three observers who participated in Experiment 1 served as subjects in this second experiment.

### 3.2. Apparatus and stimuli

Stimuli were generated and displayed by using the same apparatus as in Experiment 1. In order to measure RT accurately, an external two-buttons device was sampled every 0.5 μs by a second PC (connected to the stimuli generator PC via parallel port) from the presentation of the first frame. The method (Regan & Hamstra, 1993) allows us to establish whether or not a subject’s responses were based on trial-to-trial variations in time-to-contact or on trial-to-trial-variation in rate of expansion. We have adapted this procedure to create the comparison stimuli. The comparison stimuli were arranged in a 9 × 6 matrix, where time-to-contact varied horizontally and the ratio size to approaching velocity ( $S/v$ ) varied vertically. The six values of TC were as follows: 0.806, 0.851, 0.898, 1.114, 1.175 and 1.24 s. The TC of the standard stimuli was set to 1 s. Note that all the differences between the comparison stimuli and the standard one were above 10%. The nine values of  $S/v$  were obtained by combining three sizes (0.04, 0.05 and 0.07 m) and three constant approaching velocities (2.5, 5.0 and 10.0 ms<sup>-1</sup>). In order to uncorrelate initial rate of expansion and time-to-contact we used four different values of initial rate of expansion for the standard stimuli. Thus, for a given time-to-contact half of the comparison stimuli had a smaller initial rate of expansion than the standard and the other half had a larger one. In order to remove  $\Delta\theta$  as a reliable cue, presentation duration was varied as in Experiment 1.

### 3.3. Procedure

The psychophysical method of constant stimuli, with 2AFC, was used. Before each trial, the computer selected one of a set of 54 stimuli from the 9 × 6 matrix to be compared with the standard stimuli. Within each trial, subjects first saw an expanding square that served as the standard stimuli. After 400 ms, a second expanding square (the comparison stimuli) was shown. The 54 comparison stimuli were displayed in random order until all the stimuli had been presented. After re-randomizing, the same procedure was repeated three times within any one session. Ten sessions were carried out resulting in 30 trials per each of the 54 stimuli, 1620 responses in all. The task was to signal, by pressing one of the two buttons, which square would arrive first to the observation point. The RT was measured from the start of the presentation of the second square. The subject was required to press the button as quickly as she/he could without loss of accuracy. Auditory feed-

back was provided. Both response accuracy and RT were stored.

### 3.4. Reaction time prediction

Different RT theoretical functions can be drawn as a function of  $S/v$ , assuming that the observer initiates the response when the relevant signal generated by the comparison stimuli reaches a response threshold. This response threshold is assumed to be constant (at least within the same session and subject). If that signal corresponds with  $\tau$  or  $\tau^{-1}$ , then we expect that RT to be independent of variations in  $S/v$ , and consequently all the data points will lie along a flat curve. Another possibility is that the subject’s response is initiated when a linear weighted combination of optical size ( $\theta$ ) and rate of expansion ( $\dot{\theta}$ ) (Smith et al., 2001) reaches a threshold. Hereafter, we shall call this linear combination  $\omega_t$ , being  $\omega_t = w_s\theta_t + w_r\dot{\theta}$ . If response is triggered when  $\omega_t$  reaches a critical threshold value ( $\omega_c$ ), then RT data will be best described by

$$RT_{\omega} \approx \frac{1}{2} \frac{-w_s(S/v) + 2\omega_c T_0 - \sqrt{w_s^2(S/v)^2 + 4\omega_c w_r S/v}}{\omega_c} + t_m \tag{3}$$

where  $T_0$  is the TC of the approaching stimulus and  $t_m$  is an additive term that includes the subject’s ‘willingness to respond’ (Link, 1992) and a motor delay. The linear parameters  $w_s$  and  $w_r$  modulate the shape of Eq. (3). For large negative values of  $w_s$  Eq. (3) decreases hyperbolically with  $S/v$  given that  $w_r$  is positive. If  $w_r$  equals zero and  $w_s$  equals one then  $\omega_t$  becomes  $\omega_t = \theta_t$ . The RT function would then become linear with respect to  $S/v$ :

$$RT_{\theta} = \left[ -\frac{1}{2 \tan \theta_c} \frac{S}{v} + T_0 \right] + t_m \tag{4}$$

Therefore, if the observer initiates the response when a threshold of size  $\theta_c$  is reached the observed distribution of RT points should not significantly deviate from a line with a negative slope when they are plotted against  $S/v$ .

Alternatively, if we assume that the observer initiates the response when the comparison stimuli reaches a rate of expansion threshold  $\dot{\theta}_c$  then the RT points will be best fitted by a decreasing linear function of  $\sqrt{(S/v)}$ :

$$RT_{\dot{\theta}} \approx \left[ -\frac{\sqrt{2}}{2\sqrt{\dot{\theta}_c}} \sqrt{\frac{S}{v}} + T_0 \right] + t_m \tag{5}$$

Finally, if we assume that the observer initiates the response when a threshold ( $\eta_c$ ) of  $\eta_t$  (Eq. (1)) is reached relative to the previous standard stimulus, the predicted RT may be approximated by:

$$RT_{\eta} \approx \frac{1}{2} T_0$$

$$\begin{aligned} & \alpha 2 \arctan \left( \frac{S}{2vT_0} \right) + 2W \left( -\frac{1}{2} \frac{1}{\sqrt{\left( \frac{C}{\eta_c T_0 \alpha^2 2 \arctan \left( \frac{S}{2vT_0} \right) \right)}}} \right) \\ \times & \frac{\left( -\frac{1}{2} \frac{1}{\sqrt{\left( \frac{C}{\eta_c T_0 \alpha^2 2 \arctan \left( \frac{S}{2vT_0} \right) \right)}}} \right)}{W \left( -\frac{1}{2} \frac{1}{\sqrt{\left( \frac{C}{\eta_c T_0 \alpha^2 2 \arctan \left( \frac{S}{2vT_0} \right) \right)}}} \right)} \\ & + t_m \end{aligned} \tag{6}$$

where  $\alpha$  and  $C$  are the parameters in Eq. (1) and  $W$  is the Lambert’s function (see the Appendix A for more details). As to have a more intuitive understanding of the form of Eq. (6), it behaves like a polynomial function of the form  $a(x - b)^2 + c$ . Thus, contrary to (3), Eq. (6) is not an asymptotic function. Hence, the largest value of  $S/v$  does not necessarily correspond with the slowest response time.

In order to discern which of these theoretical functions fits the data better, we minimized a  $\chi^2$  merit function that compares the residual errors of the fit with the standard deviations in the points themselves.

### 3.5. Results

#### 3.5.1. Analysis of accuracy

Due to the fact that the differences in arrival time of the two objects were above threshold, the percentage of incorrect responses ranged from 4% to 24% depending on the  $S/v$  level and subject. The mean percentage of correct responses was 88%. Fig. 3 shows the expected pattern of correct responses for the two optical variables ( $\theta$  and  $\hat{\theta}$ ), for  $\omega$  and for  $\eta$ . The expected accuracy is plotted as a function of time within the range of the stimuli presentation duration. The observed proportion of correct responses is denoted by the horizontal dotted line. The predicted pattern of correct responses was generated as follows. For a given variable, say  $\theta_i$ , its value was computed at each time slice for both the standard and comparison stimuli. The stimulus with the largest value was chosen to be the first to arrive at the point of observation. Accuracy was incremented if the chosen stimulus had a shorter TC. Proportion of accuracy was computed over the 54 distinct stimuli at each time. The same procedure applies to the rest of functions. Neither rate of expansion nor optical size can explain the accuracy pattern (see Fig. 3). Note that the presentation duration was set randomly in the interval 440–660 ms. The mean accuracy within this range for the two optical variables was considerably lower than the observed pattern. Alternatively,  $\eta$  predicted the accuracy pattern with the closest match for the observed

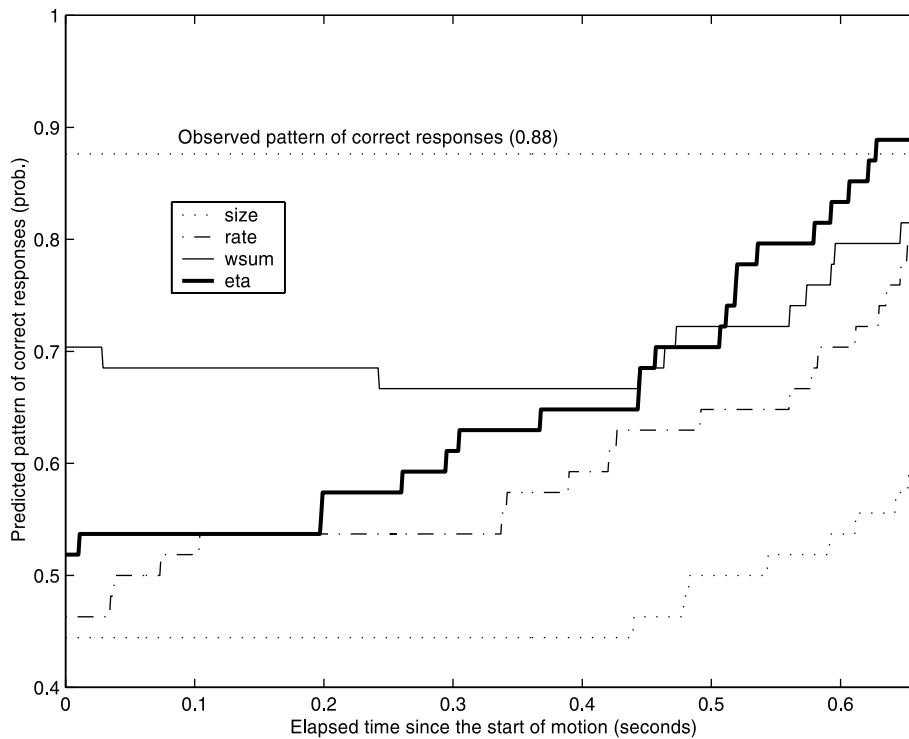


Fig. 3. Pattern of correct responses across time predicted by differences in  $\theta$ ,  $\hat{\theta}$ ,  $w_s\theta + w_r\hat{\theta}$  and  $\eta$ . The predicted proportion of accuracy is shown within the stimuli duration interval.

data. The weighted sum  $\omega$  did not substantially deviate, though, from  $\eta$  in specific intervals of the animation.

3.5.2. Reaction time analysis

Since the differences between RT (correct) and RT (correct + error) were not significant, RT analysis was performed on all the RT responses. In Fig. 4 we plot the RT (open symbols), averaged over the six TC, as a function of  $S/v$  and the fits of the RT theoretical functions (lines) to the data points. It is evident that the data are not independent of  $S/v$  so that neither  $\tau$  nor  $\tau^{-1}$  modulated the speed of the response initiation. Since the RT does not decrease linearly with  $S/v$ ,  $\theta$  itself does not seem to have a relevant role in the response initiation. Consequently, we only fitted Eqs. (3), (5) and (6) to the data points (Fig. 4).

The parameters of the three functions were estimated with the nonlinear *lsqnonlin* procedure (Levenberg–Marquardt algorithm) of the Matlab software. The re-

sults of the fits of the three RT functions are shown in Table 1. Significant values of  $\chi^2$  indicate that a given function was not a good description of the pattern in the RT data points. We can therefore reject the hypothesis that the response initiation was modulated by the flow of information corresponding to that function.

The obtained values for the different parameters of the three functions are given in Table 2. On the basis of the  $\chi^2$  values we can reject the hypothesis that the rate of expansion itself accounts for the response initiation. However, both  $RT_\omega$  and  $RT_\eta$  provided a good description of the observed RT data for the group. Looking at the individual patterns, we could only reject the weighted sum function  $RT_\omega$  for observer EN.

3.5.3. Parameter interpretation

*Expansion rate function  $RT_\theta$ .* Had the subjects' response been modulated by expansion rate, the parameter  $\theta_c$  in Eq. (5) would have shown little deviation from the

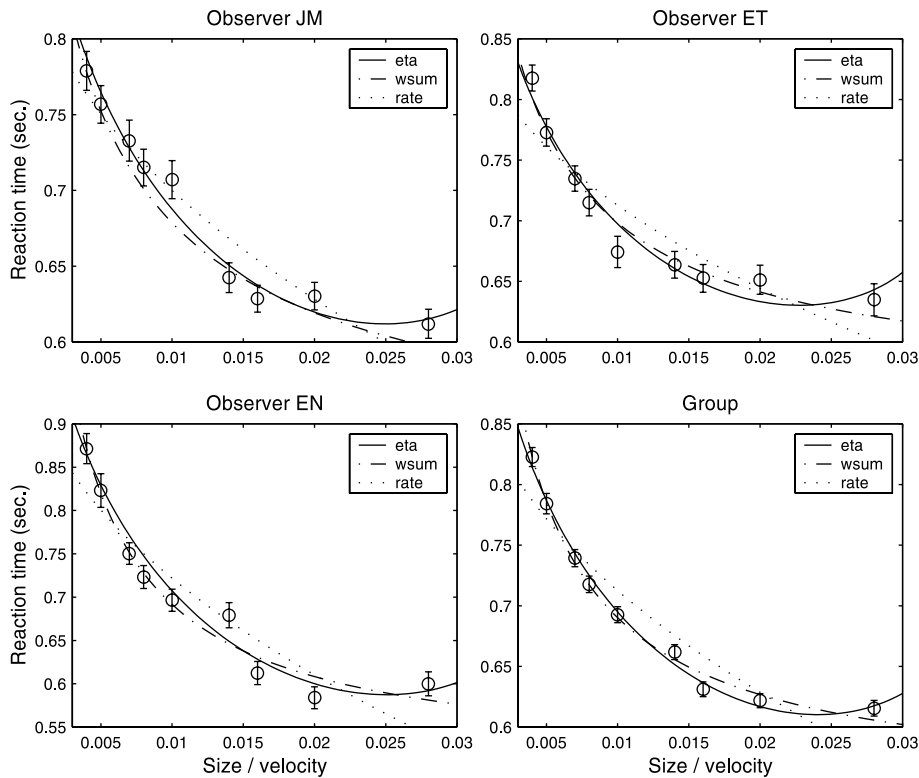


Fig. 4. Observed RT as a function of  $S/v$ . Curves are the fits of the three theoretical RT functions:  $RT_\theta$  (Eq. (5)),  $RT_\omega$  (Eq. (3)) and  $RT_\eta$  (Eq. (6)). Bars show  $\pm 1$  SE.

Table 1  
 $\chi^2$  values and their significance for the different theoretical RT functions that we have fitted to the RT data points

Observer	$RT_\theta$	$RT_\omega$	$RT_\eta$
JM	$\chi^2(6) = 25.89, p < 0.01$	$\chi^2(4) = 9.36, p = 0.053$	$\chi^2(4) = 6.26, p = 0.181$
ET	$\chi^2(6) = 40.15, p < 0.01$	$\chi^2(4) = 8.12, p = 0.087$	$\chi^2(4) = 9.21, p = 0.056$
EN	$\chi^2(6) = 40.20, p < 0.01$	$\chi^2(4) = 10.65, p = 0.031$	$\chi^2(4) = 9.07, p = 0.060$
Group	$\chi^2(6) = 100, p < 0.01$	$\chi^2(4) = 8.99, p = 0.061$	$\chi^2(4) = 7.07, p = 0.132$

Table 2

Parameter estimates obtained by fitting the theoretical functions to the observed RT data points

Observer	RT $_{\theta}$			RT $_{\omega}$					RT $_{\eta}$				
	$\dot{\theta}_t$ (rads $^{-1}$ )	$T_0$ (s)	$t_m$ (s)	$w_s$	$w_r$	$\dot{\theta}_t$	$T_0$	$t_m$	$\alpha$	$C$	$\eta_t$	$T_0$ (s)	$t_m$ (s)
JM	0.18	0.75	0.116	-2.86	1.94	0.016	1.08	0.120	16.57	1.91	0.10	0.91	0.115
ET	0.16	0.72	0.173	-2.38	1.80	0.010	1.15	0.165	18.66	1.76	0.08	0.92	0.135
EN	0.08	0.76	0.207	-1.46	2.58	0.001	2.03	0.234	25.99	0.94	0.02	1.00	0.235
Group	0.13	0.71	0.197	-1.95	2.39	0.002	1.56	0.208	20.38	1.87	0.07	0.95	0.152

mean expansion rate at the time when the subjects responded. However, the estimates were always much larger than the expansion rate at the response time for all the observers and for the group. The mean expansion rate at the response time was about 0.057 rads $^{-1}$ . We took into account the estimated motor delay ( $t_m$ ) to compute this value. Interestingly, only for the less trained observer (EN) the threshold estimate  $\dot{\theta}_c$  did not substantially deviate from the value that the expansion rate would predict (0.077 versus 0.025 rads $^{-1}$ ). However, on the basis of the poor fit and the observed pattern of accuracy, we can rule out the possibility that  $\dot{\theta}$  was responsible for the response initiation.

*Weighted sum function* RT $_{\omega}$ . Because of the large number of parameters in Eqs. (3) and (6) and in order to avoid spurious mathematical fits, we had to guarantee the functional significance of the obtained parameter values. To do this, we fitted Eq. (3) to a set of points that simulated a response initiated when a weighted combination of  $\theta$  and  $\dot{\theta}$  reached a certain value. In order to generate the points, we used several combinations of  $w_s$ ,  $w_r$  and  $\omega_c$ . Similarly, we used different values of  $\alpha$ ,  $\eta_c$ ,  $C$ ,  $T_0$  and  $t_m$  to simulate the time values that would be generated by Eq. (6). The estimated parameters always matched the values used for generating the data points. The fit therefore did not merely reflect a mathematical fact.

As stated in Section 3.5.2 and on the basis of the goodness of fit, we cannot reject the hypothesis that the observers initiated the response when a critical value (response threshold) of  $\omega_t$  was reached. In order for Eq. (3) to accurately fit the data points,  $w_s$  should converge to a negative value. This fact is consistent with the inhibitory role of  $\theta$  in  $\eta_t$  (Eq. (1)). Therefore, the role of  $w_s$  would be essentially similar to the role of  $\alpha$  in Eq. (1). The fit for observer EN yielded the lowest  $w_s$  relative to  $w_r$ , ( $w_s/w_r = -0.57$ ). For the more trained observers JM and ET this ratio was -1.47 and -1.32 respectively, suggesting that  $\theta$  was more used and combined with  $\dot{\theta}$  to respond. This pattern is consistent with that reported by Smith et al. (2001). These authors showed that, with practice, observers learned to combine optical size and its rate of expansion, whereas the data early in practice only reflected an expansion rate strategy. Since we can know the  $\theta$  and  $\dot{\theta}$  values of the stimuli at the response time, we can compute the value of  $\omega_t$  by using the

estimates for  $w_s$  and  $w_r$ . Hence, not only can we know the value of the weighted sum function  $\omega_t$  but also we can compare it with the estimated threshold ( $\omega_c$  in Eq. (3)). However, the fitted threshold parameter  $\omega_c$  was smaller than the value of  $\omega_t$  at the mean response time. For example,  $\omega_t$  yielded a value about 0.0873 ( $-1.95 \times 0.025 \text{ rad} + 2.39 \times 0.057 \text{ rads}^{-1}$ ) for the group, while the estimated value ( $\omega_c$ ) was 0.0024 (see Table 2). We can nevertheless give a possible explanation for this underestimation. RT $_{\omega}$  was fitted to the RT data averaged over the six TC values. Therefore, a solution reflecting a tradeoff among the six TC values would necessarily underestimate  $\theta$  and  $\dot{\theta}$ , because the mean expansion rate (or size) is substantially larger than expansion rate (or size) of the mean TC.

*$\eta$  function* RT $_{\eta}$ . As before, we first guaranteed that the obtained values of the parameters reflected plausible solutions. The  $\alpha$  parameter (see Table 2) ranged from about 16 for observers JM and ET to 27 for observer EN. The slope of the ascending phase of the  $\eta$  function is shallower for larger  $\alpha$  values, so  $\eta$  signal would grow at a lower rate towards the response threshold. These values were consistent with the slower mean RT for observer EN.

Because  $\eta$  (Eq. (1)) is scaled by  $C$ , the estimated  $\eta_c$  threshold (parameter  $\eta_c$ ) in Eq. (6) cannot be directly compared as a response threshold. However, the ratio of  $\eta_c$  to  $C$  was very similar for observers JM and ET (0.05 and 0.046), while for observer ET was 0.02. Although a threshold of 0.02 would have elicited a faster response than 0.05, the former was reached at a lower rate because of the larger  $\alpha$ . As before, the values of the estimated parameter  $\eta_c$  in Eq. (6) can be compared with the mean value of the  $\eta_t$  function (Eq. (1)) at the response time minus the estimated motor delay  $t_m$ . We computed these values for the different observers and for the group using the corresponding  $\alpha$  and  $C$  estimates. If we plot the predicted  $\eta_t$  values against the  $\eta_c$  threshold estimates we would ideally expect a linear relationship with a slope of one and intercept of zero. Fig. 5 shows this linear fit. The 95% confidence interval for the slope and intercept ranged from 0.6657 to 1.0756, and from -0.002 to 0.014 respectively, so both intervals include the expected values.

The parameter  $T_0$  should ideally be close to 1 s. since the comparison stimuli have a mean value of TC set to



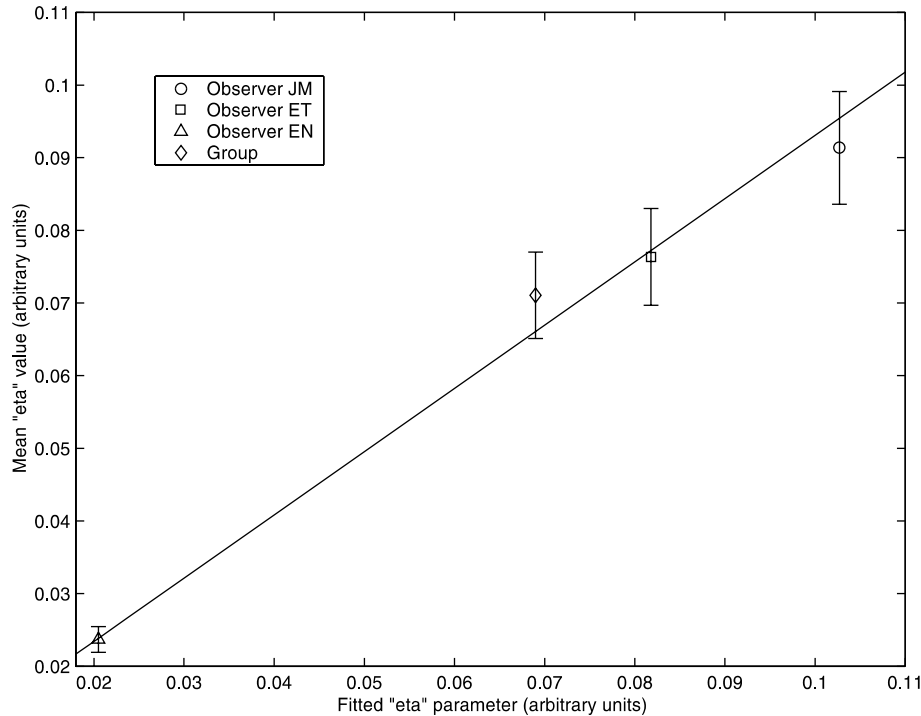


Fig. 5. The mean value of the  $\eta_i$  function (Eq. (1)) computed at the response time against the  $\eta_c$  threshold as estimated by the fit. The value of  $\eta_i$  is the average over all the comparison stimuli. For each observer and for the group we used the corresponding values of  $\alpha$  and  $C$ . The line is the best fit to the four points. Bars show  $\pm 1$  SE. See text for details.

1 s. As can be noted, the estimated  $T_0$  closely resembled the theoretical value (0.95 s for the group). This value was a little bit smaller for the two-trained subjects (JM and ET). Finally, a quantity of the observed RT should be related to a response criterion that would include a motor delay. The term  $t_m$  in Eq. (5) represents the duration of this component. Like  $T_0$ , the estimates were smaller for the trained subjects (0.115 s for JM and 0.134 s for ET) than for the less trained one (0.235 s for EN). Admittedly, we might expect a larger value for  $t_m$ , but due to the fact that the estimates were slower for the trained subjects,  $t_m$  could also reflect decisional processes that are indeed sensible to training. It has proven that response threshold (or response criterion) decreases with training when choice RT is used (Bonnet & Dresch, 2001).

#### 4. Discussion

Experiment 2 provides empirical support for a measurement of TC based on the computation of  $\eta$ . The differences in  $\eta$  between the standard and comparison stimuli signal the correct response more accurately than the differences in rate of expansion, optical size or a weighted sum of the two optical variables (see Fig. 3). This superiority in the predicted accuracy holds to about 200 ms before the contact. That is to say, visual infor-

mation provided by  $\eta$  appears to be more useful during the most relevant part of the trajectory, 250–300 ms before the contact (Whiting & Sharp, 1974). Expansion rate reaches its maximum accuracy less than 200 ms ahead and the predicted accuracy was less than 80% during the last part of the displayed animation. Had the observers' responses been modulated by an expansion rate strategy the observed percentage of correct responses would have been significantly lower. Although the weighted sum model deviates from the observed pattern less than expansion rate or size, it can hardly account for the overall proportion of accuracy. However, the linear parameters  $w_s$  and  $w_r$  could have been tuned to fit the requirements of a RT task instead of a pure discrimination task. This would be one of the key features of the weighted sum model (Smith et al., 2001).

Similarly, the type of combination between  $\theta$  and  $\hat{\theta}$  specified by  $\eta$  could also be tuned according to the task demands.  $\alpha$  and  $C$  parameter could thus behave in a flexible way. As our data suggests, extensive psychophysical training could result in changes of  $\alpha$ .  $\alpha$  values were similar for the two more trained participants. Additional fits for early and late sessions, however, failed to yield significant differences for any observer. This lack of difference between early and late sessions is easy to explain for the two more trained subjects due to their extensive training at the beginning of the experiments. Although the less trained subject took three

previous sessions of training, this was not so extensive at the beginning of the experiments. We do not know whether or not more training would produce a noticeable change. If so, there would be little practical difference between  $\eta$  and  $\omega$ . Alternatively,  $\eta$  could be reflecting a kind of hard-wired mechanism so that different  $\alpha$  values would thus suggest sensory differences. Since we did not design our studies to address this issue, further experiments are needed to clarify this point.

However, regardless of the nature of the mechanism, a valuable property of a TC signal is that it should allow discriminating small differences as collision approaches (Tresilian, 1999). As predicted by Weber's law, if the signal grows proportionally with "contact immediacy", then small differences are more difficult to discriminate. Unlike  $\omega$ ,  $\eta$  shows a drop-off before collision allowing discriminations that would be hardly achieved otherwise.

Further explorations of the use of  $\eta$  should be extended to tasks involving performance of actions that require a very precise timing. Note that in Experiment 2, the observers are not required to respond at any precise time. The fact that  $\eta$ 's signal shows a peak before the collision could be useful for starting an interceptive or avoiding action. However, the peak corresponds with a particular visual angle for a given  $\alpha$  value and it is not clear how the image of a large object that is far away and that of a small object that is near are unconfounded. Thus, whether or not  $\eta$  plays a relevant role in motion initiation when timing constraints are very stringent is an open question. Related to this, none of the neurons studied by Sun and Frost (1998) responded to simulated self-motion to stationary objects. This raises the question whether the computation of  $\eta$  can be carried on from the divergence of optic flow or from changes in the size of the image. Recently, Schrater, Knill, and Simoncelli (2001) have shown that visual expansion can be estimated without optic flow.

The experiments reported here have only addressed monocular optical variables. Future models of timing action should consider how the computation of monocular information (e.g.  $\eta$  and  $\omega$ ) is combined with binocular cues of time-to-contact. In respect of this issue, the *dipole model* (Rushton & Wann, 1999) could provide for the necessary theoretical bounds in order to design future experiments.

### Acknowledgements

We are grateful to Allan Pantle, John Flach and Leonard Mark for useful comments on an earlier version of this article. We also thank Rob Gray and Roy Davis for a number of important suggestions, Diego Alonso and Enrique Romero for their mathematical assistance and Elisabet Tubau and Eduardo Navarrete

for their active participation. This research was supported, in part, by the Ministerio de Ciencia y Tecnología of the Spanish government, grant number BSO 2001–2008.

### Appendix A. Mathematical appendix

Let  $S$  denote an object's diameter that approaches an observer at constant velocity  $v$ , at time  $t$  the object subtends a semiangle  $\theta_t$  and its rate of expansion is  $\dot{\theta}_t$ . Let  $T_0$  be the time-to-contact ( $TC$ ) at the beginning of the motion, that is at time  $t = 0$ ; let  $t$  be the time when the optical variable threshold is reached and  $t_m$  the decisional and motor latency. Thus, the RT would be expressed as  $RT = t + t_m$ .

It has been shown (Sun & Frost, 1998) that the distribution of response onset holds different relationships with  $S/v$  depending on the type of looming-detector. Following the same rationale, we can predict the shape of the RT distribution assuming that the response is triggered when a threshold value of an optical variable is reached.

#### A.1. Reaction time function when $\omega_t$ reaches a threshold value

The update of the tangent of the semiangle subtended by the object at any time can be approximated by

$$\tan \theta_t = \frac{\tan \theta_0}{1 - t/T_0} \quad (\text{A.1})$$

where  $\theta_0$  is the object's semiangular subtense at time  $t = 0$ . If we differentiate with time (A.1), we obtain an expression for the expansion rate

$$\dot{\theta}_t = \frac{\tan \theta_0}{\left(1 - \frac{t}{T_0}\right)^2 T_0 \left(1 + \frac{(\tan \theta_0)^2}{\left(1 - \frac{t}{T_0}\right)^2}\right)} \quad (\text{A.2})$$

since in our case

$$\frac{[\tan \theta_0]^2}{\left(1 - \frac{t}{T_0}\right)^2} \ll 0.005 \quad (\text{A.3})$$

the rate of expansion of the angle  $\theta$  can be approximated at time  $t$  by:

$$\dot{\theta}_t \approx \frac{\tan \theta_0}{\left(1 - \frac{t}{T_0}\right)^2 T_0} \quad (\text{A.4})$$

The weighted sum function  $\omega$  is therefore defined at time  $t$  as:

$$\omega_t \approx w_s \left[ \frac{\tan \theta_0}{1 - t/T_0} \right] + w_r \left[ \frac{\tan \theta_0}{\left(1 - \frac{t}{T_0}\right)^2 T_0} \right] \quad (\text{A.5})$$

Because this is a monotonic function in the interval  $[0, T_0]$  we can easily obtain a value of  $t$  for a given threshold  $\omega_t$ :

$$\frac{\tan \theta_0 T_0 (w_s T_0 - w_s t + w_r)}{(T - t)^2} = \omega_t \quad (\text{A.6})$$

$$\frac{w_s T_0 - w_s t + w_r}{(T_0 - t)^2} = \frac{\omega_t}{\tan \theta_0 T_0} \quad (\text{A.7})$$

finally,

$$t \approx \frac{1}{2} \frac{-\tan \theta_0 T_0 w_s + 2\omega_t T_0 + \sqrt{(\tan \theta_0)^2 T_0^2 w_s^2 + 4\omega_t \tan \theta_0 T_0 w_r}}{\omega_t} \quad (\text{A.8})$$

Since

$$\tan \theta_0 = \frac{S}{2vT_0} \quad (\text{A.9})$$

We can express  $t$  as a function of  $S/v$ :

$$t \approx \frac{1}{2} \frac{-w_s S/v + 2\omega_t T_0 - \sqrt{w_s^2 S/v^2 + 4\omega_t w_r S/v}}{\omega_t} \quad (\text{A.10})$$

Thus, if the response is initiated when a threshold  $\omega_c$  is reached, then the theoretical RT function predicted by the weighted sum model is

$$\text{RT}_\omega \approx \frac{1}{2} \frac{-w_s S/v + 2\omega_c T_0 - \sqrt{w_s^2 S/v^2 + 4\omega_c w_r S/v}}{\omega_c} + t_m \quad (\text{A.11})$$

*A.2. Reaction time function when  $\theta_t$  reaches a threshold value*

From expression (A.11) we can easily derive the RT function when  $\theta_t$  reaches a critical value  $\theta_c$ . If we let  $w_s = 1$  and  $w_r = 0$ , and substituting  $\omega_t$  for  $\tan \theta_c$ , it is easy to show that the theoretical RT function for  $\theta$  is

$$\text{RT}_\theta = \left[ -\frac{1}{2 \tan \theta_c} \frac{S}{v} + T_0 \right] + t_m \quad (\text{A.12})$$

The RT should therefore decrease linearly with  $S/v$  if the observer responds when a certain value of  $\theta_t$  is reached.

*A.3. Reaction time function when  $\dot{\theta}_t$  reaches a threshold value*

Similarly, we can use the same rationale to derive the RT function when  $\dot{\theta}_t$  reaches a critical threshold  $\dot{\theta}_c$ . Let  $w_s = 0$  and  $w_r = 1$  and substituting  $\omega_c$  for  $\dot{\theta}_c$

$$\text{RT}_{\dot{\theta}} \approx \left[ -\frac{\sqrt{2}}{2\sqrt{\dot{\theta}_c}} \sqrt{\frac{S}{v}} + T_0 \right] + t_m \quad (\text{A.13})$$

Thus, the RT should have a linear relationship with  $\sqrt{S/v}$ .

*A.4. Reaction time distribution when  $\eta$  reaches a threshold value*

Because the  $\eta_t$  function is not monotonic, it is not straightforward to obtain an inverse function. However, it is possible to have an analytic expression that gives us a solution to  $t$  assuming that the response is initiated before  $\eta_t$  reaches peak value.

From now on, let us  $\theta_0$  denote the object's angular subtense at time  $t = 0$  rather than the semiangle. The optical size can be updated according to  $\theta_t = \theta_0 / (1 - t/T_0)$  instead of (A.1) when both  $\theta_0$  and  $\theta_t$  are small (Gray & Regan, 1998), in our case the maximum error in the displayed angle is less than 0.006%. Thus,  $\eta_t$  can be approximated by using the following expression:

$$\eta_t \approx C \frac{\theta_0}{\left(1 - \frac{t}{T_0}\right)^2 T_0} e^{-\alpha \frac{\theta_0}{1-t/T_0}} \quad (\text{A.14})$$

and

$$\frac{e^{\left(\frac{-\alpha \times \theta_0}{(1-t/T_0)}\right)}}{(1-t/T_0)^2} = \frac{\eta_t T_0}{\theta_0 C} \quad (\text{A.15})$$

$$\frac{T_0^2 e^{\left(\frac{-\alpha \theta_0}{(1-t/T_0)}\right)}}{(-T_0 + t)^2} = \frac{\eta_t T_0}{\theta_0 C} \quad (\text{A.16})$$

$$\frac{e^{\left(\frac{-\alpha \theta_0}{(1-t/T_0)}\right)}}{(-T_0 + t)^2} = \frac{\eta_t}{\theta_0 C T_0} \quad (\text{A.17})$$

Because Eq. (A.17) involves transcendental functions, a solution for variable  $t$  cannot be obtained in terms of known functions. However, it is possible to obtain an accurate approximation by using Lambert's  $W(x)$  function (Jeffrey & Knuth, 1996), where  $y = W(x)$  is the solution to  $y \times \exp(y) = x$ . Thus a solution to (A.17) in terms of  $W(x)$  is:

$$t \approx \frac{1}{2} T_0 \frac{\alpha \theta_0 + 2W \left( -\frac{1}{2} \frac{1}{\sqrt{\frac{C}{\eta_t T_0 \alpha^2 \theta_0}}} \right)}{W \left( -\frac{1}{2} \frac{1}{\sqrt{\frac{C}{\eta_t T_0 \alpha^2 \theta_0}}} \right)} \quad (\text{A.18})$$

Thus, the RT when  $\eta_t$  has reached a threshold value  $\eta_c$  would be approximated by:

$$\text{RT}_{\eta} \approx \frac{1}{2} T_0 \times \frac{\alpha 2 \arctan \left( \frac{s}{2vT_0} \right) + 2W \left( -\frac{1}{2} \frac{1}{\sqrt{\left( \frac{C}{\eta_c T_0 \alpha^2 2 \arctan \left( \frac{s}{2vT_0} \right)} \right)}} \right)}{W \left( -\frac{1}{2} \frac{1}{\sqrt{\left( \frac{C}{\eta_c T_0 \alpha^2 2 \arctan \left( \frac{s}{2vT_0} \right)} \right)}} \right)} + t_m \quad (\text{A.19})$$

It is possible to obtain numerical values of  $W(x)$  by using Newton's method. We used the Maple's implementation of the  $W$  function, so that having  $W$  in Eq. (A.19) is not a problem from a practical point of view.

## References

- Bonnet, C., & Dresch, B. (2001). Reaction time studies of sensory magnitude and perceptual processing. *Psychologica*, 28, 63–86.
- DeLucia, P. (1991). Pictorial and motion based information for depth perception. *Journal of Experimental Psychology: Human, Perception and Performance*, 17, 738–748.
- DeLucia, P. (1999). Size-arrival effects: the potential roles of conflicts between monocular and binocular time-to-contact information, and of computer aliasing. *Perception & Psychophysics*, 61, 1168–1177.
- Gray, R. (2000). Attentional modulation of motion-in-depth processing. *Vision Research*, 40, 1041–1050.
- Gray, R., & Regan, D. (1998). Accuracy of estimating time to collision using binocular and monocular information. *Vision Research*, 38, 499–512.
- Hanes, D., & Schall, J. (1996). Neural control of voluntary movement initiation. *Science*, 274, 427–430.
- Hatsopoulos, N., Gabbiani, F., & Laurent, G. (1995). Elementary computation of object approach by a wide-field visual neuron. *Science*, 270, 1000–1003.
- Jeffrey, D. J., & Knuth, D. E. (1996). On the lambert  $w$  function. *Advances in Computational Mathematics*, 5, 329–359.
- Kaernbach, C. (1991). Simple adaptive testing with the weighted up-down method. *Perception & Psychophysics*, 49, 227–229.
- Kerzel, D., Hecht, H., & Kim, N. (1999). Image velocity, not tau, explains arrival-time judgements from global optical flow. *Journal of Experimental Psychology: Human Perception and Performance*, 25, 1540–1555.
- Koenderink, J. J. (1985). Brain mechanisms and spatial Vision. In D. Ingle, M. Jeannerod, D. Lee (eds.), *Space, form and optical deformations* (pp. 31–59). Norwood, NJ: Martinus Nijhoff Publishers.
- Laurent, G., & Gabbiani, F. (1998). Collision-avoidance: nature's many solutions. *Nature Neuroscience*, 1, 261–263.
- Link, S. W. (1992). *The wave theory of discrimination and similarity*. Hillsdale, NJ: Erlbaum.
- Pins, D., & Bonnet, C. (1996). On the relation between stimulus intensity and processing time: Piéron's law and choice reaction time. *Perception & Psychophysics*, 58, 390–400.
- Pins, D., & Bonnet, C. (2000). The Piéron function in the threshold region. *Perception & Psychophysics*, 62, 127–136.
- Regan, D., & Hamstra, S. J. (1993). Dissociation of discrimination thresholds for time to contact and for rate of angular expansion. *Vision Research*, 33, 447–462.
- Regan, D., & Vincent, A. (1995). Visual processing of looming and time to contact throughout the visual field. *Vision Research*, 35, 1845–1857.
- Rushton, S., & Wann, J. (1999). Weighted combination of size and disparity: a computational model for timing a ball catch. *Nature Neuroscience*, 2, 186–190.
- Schrater, P., Knill, D., & Simoncelli, E. (2001). Perceiving visual expansion without optic flow. *Nature*, 410, 816–819.
- Smeets, J., Brenner, E., Trébuchet, S., & Mestre, D. (1996). Is time-to-collision perception based on tau? *Perception*, 25, 583–590.
- Smith, M., Flach, J., Dittman, S., & Stanard, T. (2001). Monocular optical constraints on collision control. *Journal of Experimental Psychology: Human Perception and Performance*, 27, 395–410.
- Sun, H., & Frost, B. J. (1998). Computation of different optical variables of looming objects in pigeon nucleus rotundus neurons. *Nature Neuroscience*, 1, 296–303.
- Todd, J. T. (1981). Visual information about moving objects. *Journal of Experimental Psychology: Human Perception and Performance*, 7, 795–810.
- Tresilian, J. R. (1995). Perceptual and cognitive processes in time-to-contact estimation: analysis of prediction-motion and relative judgement tasks. *Perception and Psychophysics*, 57, 231–245.
- Tresilian, J. R. (1999). Visually timed action: time-out for tau? *Trends in Cognitive Science*, 3, 301–309.
- Wann, J. (1996). Anticipating arrival: is the tau-margin a specious theory? *Journal of Experimental Psychology: Human Perception and Performance*, 22, 1031–1048.
- Whiting, H., & Sharp, R. (1974). Visual occlusion factors in a discrete ball-catching task. *Journal of Motor Behavior*, 6, 11–16.